J Biomol NMR (2008) 40:175–181
DOI 10.1007/s10858-008-9219-5

ARTICLE

Projected [^{1}H,^{15}N]-HMQC-[^{1}H,^{1}H]-NOESY for large molecular systems: application to a 121 kDa protein-DNA complex

Veniamin Galius · Chrysoula Leontiou · Timothy Richmond · Gerhard Wider

Received: 29 October 2007 / Accepted: 8 January 2008 / Published online: 30 January 2008

Abstract We present a projected [^{1}H,^{15}N]-HMQC-[^{1}H,^{1}H]-NOESY experiment for observation of NOE interactions between amide protons with degenerate ^{15}N chemical shifts in large molecular systems. The projection is achieved by simultaneous evolution of the multiple quantum coherence of the nitrogen spin and the attached proton spin. In this way NOE signals can be separated from direct-correlation peaks also in spectra with low resolution by fully exploiting both ^{1}H and ^{15}N frequency differences, such that sensitivity can be increased by using short maximum evolution times. The sensitivity of the experiment is not dependent on the projection angle for projections up to 45° and no additional pulses or delays are required as compared to the conventional 2D [^{1}H,^{15}N]-HMQC-NOESY. The experiment provides two distinct 2D spectra corresponding to the positive and negative angle projections, respectively. With a linear combination of 1D cross-sections from the two projections the unavoidable sensitivity loss in projection spectra can be compensated for each particular NOE interaction. We demonstrate the application of the novel projection experiment for the observation of an NOE interaction between two sequential glycines with degenerate ^{15}N chemical shifts in a 121.3 kDa complex of the linker H1 histone protein with a 152 bp linear DNA.

Keywords HMQC · NOESY · Reduced dimensionality · Projection spectroscopy · Histone H1 · Resolution enhancement

V. Galius · C. Leontiou · T. Richmond · G. Wider (✉)
Institute of Molecular Biology and Biophysics, ETH Zurich, 8093 Zurich, Switzerland
e-mail: gsw@mol.biol.ethz.ch

Introduction

In the last 20 years NMR has found widespread applications in structural and dynamic studies of biological macromolecules with molecular weights up to about 30 kDa. More recently, NMR applications were extended to larger molecular systems where studies of local interactions and the characterization of the dynamic behavior are of prime interest and not a complete three-dimensional structure determination; usually an X-ray structure of these systems is available (Christodoulou et al. 2004; Fiaux et al. 2002; Horst et al. 2005; Sprangers and Kay 2007). This approach is a direct consequence of the fact that normally only flexible parts of the macromolecular complexes, e.g. the smaller ligand or mobile residues on the surface, are accessible to direct observation by NMR. The observable resonances often suffer from dynamic line broadening and poor spectral dispersion. For optimal sensitivity short low dimensional pulse sequences have to be used, but at the same time the spectral separation of signals must be maximized. A solution to these seemingly contradictory demands could be provided by reduced dimensionality experiments (Kupče and Freeman 2003; Szyperski et al. 1993b).

For very large molecular systems through-bond correlation experiments become very inefficient; at the same time, through-space NOE correlations do not suffer from this limitation (Horst et al. 2006). For a reduction of transverse relaxation, carbon-bound protons are often exchanged for deuterons making the observation of NOEs between nitrogen-bound protons an important source of information. The NOEs can, e.g., be used to obtain specific assignments in very large molecular structures (Horst et al. 2006). For optimal sensitivity, usually the lowest possible dimensionality of the experiments is used which may

dramatically increase the problem of spectral overlap. For example, in a 2-dimensional (2D) ^{15}N-resolved [^{1}H,^{1}H]-NOESY spectrum NOEs between protons attached to ^{15}N nuclei with similar chemical shifts cannot be observed, because they overlap with the very strong direct-correlation peaks. Further, resolved NOE crosspeaks often cannot be unambiguously assigned to a proton pair in 2D ^{15}N-resolved NOESY spectra when the attached nitrogen nuclei have degenerate chemical shifts and the transposed NOE-cross peak is not observable because of overlap. As a solution for these kind of problems, we propose a projected [^{1}H,^{15}N]-HMQC-[^{1}H,^{1}H]-NOESY experiment optimized for use with large molecular structures. In the resulting spectrum amide resonances with degenerate ^{15}N-shifts but distinct ^{1}H-shifts become separated in the indirect dimension such that NOE-crosspeaks between them can be observed.

Projection spectroscopy uses simultaneous evolution periods on different nuclei, a technique that was originally introduced for reduced dimensionality spectroscopy (Szyperski et al. 1993a, b). In recent years, several implementations of this concept have found their application: G-matrix NMR (Kim and Szyperski 2003; Kozminski and Zhukov 2003; Szyperski et al. 1993b), projection-reconstruction spectroscopy (Kupče and Freeman 2003), HIFI NMR (Eghbalnia et al. 2005), automated projection spectroscopy (APSY) (Hiller et al. 2005a) and multi-way decomposition (Malmodin and Billeter 2005). The same principle can be used for the reduction of peak overlap in lower-dimensional spectra, like the TILT experiment where ^{15}N- (Kupče and Freeman 2005) or ^{13}C-evolution periods (Kupče et al. 2005) were incremented simultaneously with a ^{1}H-evolution period. This was achieved by adding a HSQC-type polarization transfer and an additional evolution period on the heteronucleus to a homonuclear [^{1}H,^{1}H]-NOESY experiment. The same concept was utilized for maximizing the number of resolved amide resonances in a ^{15}N-$T_{1\rho}$-relaxation experiment (Tugarinov et al. 2004) by projecting the ^{15}N and the carbonyl frequencies onto one axis.

For high molecular weight systems we propose a relaxation optimized HMQC-type projection experiment that does not require any additional delays compared to the conventional 2D [^{1}H,^{15}N]-HMQC-NOESY sequence (Shon and Opella 1989). Thus, the extent of transverse relaxation during the experiment is not dependent on the selected projection angle for $0° \leq \alpha \leq 45°$ and the additional resolution can be obtained without any signal loss compared to the standard 2D version of the experiment. Further, the resolution obtained in the indirect dimension is higher than would be affordable in a corresponding three-dimensional (3D) experiment. The experiment can either be used to resolve particular pairs of NOE-signals, or to provide a 2D [^{1}H,^{15}N]-HMQC-[^{1}H,^{1}H]-NOESY spectrum with a maximum number of unambiguous non-overlapped NOE-correlations. The projection angle can be optimized based on amide chemical shifts from a 2D [^{1}H,^{15}N]-correlation experiment. The experiment introduced in this paper is especially useful for high molecular weight systems and we demonstrate its application for the observation of a weak NOE-interaction between two amide protons of the H1 linker histone protein within a 121.3 kDa complex with a 152 bp linear DNA duplex.

Methods

NOEs between amide resonances with degenerate ^{15}N-shifts but distinct ^{1}H-shifts can be resolved with the proposed projected [^{1}H,^{15}N]-HMQC-[^{1}H,^{1}H]-NOESY. This experiment is based on a conventional 2D [^{1}H,^{15}N]-HMQC-NOESY (Shon and Opella 1989) and delivers a 2D spectrum corresponding to a geometric projection of a 3D ^{15}N-resolved [^{1}H,^{1}H]-NOESY spectrum on a plane spanned by the ^{1}H acquisition frequency axis and a mixed frequency axis (projected dimension (Kupče and Freeman 2003)) inclined at an arbitrary angle α between the $^{1}H^{N}$ and $^{15}N^{H}$ axes. The projected dimension is obtained by keeping the t_2(^{1}H) and t_1(^{15}N) evolution time increments at the constant ratio $\tan \alpha = \Delta t_2/\Delta t_1$ (Szyperski et al. 1993b). The HMQC pulse sequence is ideally suited for performing simultaneous ^{15}N and ^{1}H evolution during the double quantum state eliminating the need for any additional pulses or delays (Szyperski et al. 1993a). The relaxation during the joint evolution is not dependent on the projection angle α for $\alpha \leq 45°$, it depends only on the desired maximum evolution time of the ^{15}N-magnetization. When the single quantum transfer periods are used for additional constant-time proton evolution (Grzesiek and Bax 1993), the projection angle can be increased over 45° without a concomitant increase in transverse relaxation until the difference between the required maximum proton and nitrogen evolution periods exceeds the H–N transfer period. Simultaneous evolution in the multiple-quantum state in ^{1}H–^{15}N and ^{1}H–^{13}C spin pairs has been used earlier for optimizing relaxation in experiments which require independent evolution of proton and a heteronuclear coherence (Bazzo et al. 2001; Pervushin and Eletsky 2003; Ying et al. 2007).

Figure 1 shows the pulse sequence of the projected [^{1}H,^{15}N]-HMQC-NOESY with simultaneously incremented ^{1}H and ^{15}N evolution periods. According to the projection theorem (Bracewell 1956; Nagayama et al. 1978) the resulting spectrum corresponds to a geometric projection of a ^{15}N-resolved 3D [^{1}H,^{1}H]-NOESY experiment onto a plane with the ^{15}N axis tilted at the angle α

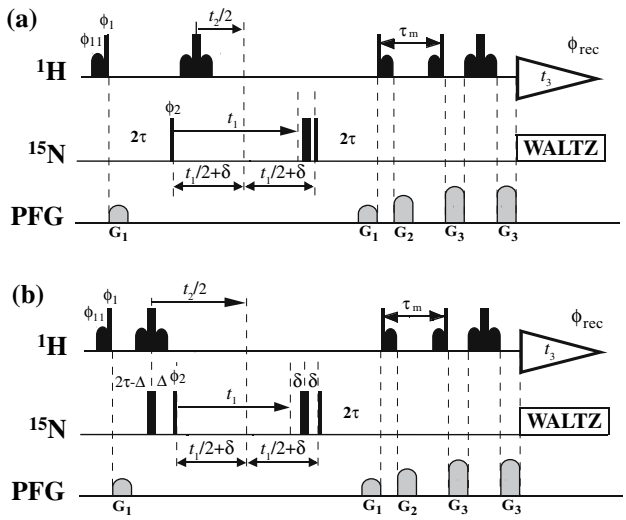

◀**Fig. 1** Pulse sequences for the 2D projected 3D [^{1}H,^{15}N]-HMQC-[^{1}H,^{1}H]-NOESY experiment for projection angles (**a**) $0° \leq \alpha \leq 45°$ and (**b**) $45° < \alpha \leq 90°$. Narrow and wide black vertical bars on the lines marked ^{1}H and ^{15}N denote 90° and 180° pulses, respectively, applied at the proton (line ^{1}H) and at the nitrogen frequency (line ^{15}N). The black bell shapes on the line ^{1}H represent gauss-shaped selective 90° pulses on the water resonance keeping the water magnetization along the +z-axis during the whole sequence. The grey bell shapes on the line PFG are sine bell shaped pulsed magnetic field gradients applied along the z-axis with the following durations and strengths: G_1, 600 µs, 30 G/cm; G_2, 700 µs, 50 G/cm; G_3, 1000 µs, 50 G/cm. The radio-frequency pulses are applied with phase x unless indicated otherwise above the pulse bar; the following phase cycles are used: φ_1 = x, x, −x, −x, $\varphi_{11} = -\varphi_1$; φ_2 = x, −x; φ_{rec} = x, −x, −x, x. In (**b**) the first refocusing pulse on ^{15}N is additionally cycled with φ_3 = −x, −x, x, x. The ^{1}H carrier frequency can be set on the water resonance throughout the whole experiment or, when the sweep width in the indirect dimension should be minimized, switched between the middle of the amide region and the water resonance at the beginning of the experiment and during the mixing time, respectively. The two sub-spectra for the projection angle α are recorded interleaved with a constant phase offset of 90° for phase φ_1 and −90° for phase φ_2. Quadrature detection in t_1 is achieved for each sub-spectrum by incrementing the pulse phase φ_2 following the STATES-TPPI scheme. The +α and −α projection spectra are then obtained from sum and difference of the two time domain data sets, respectively, according to the trigonometric addition theorem (Brutscher et al. 1995; Kupče and Freeman 2004). The evolution times t_1 (^{15}N) and t_2 (^{1}H) are incremented simultaneously at a constant ratio of $\Delta t_2/\Delta t_1$, which defines the projection angle $\alpha = \arctan(\Delta t_2/\Delta t_1)$. The following time periods are used in both pulse sequences: $\tau = 1/4J_{HN}$ and τ_m = NOESY mixing time. (**a**) refocusing the ^{15}N-chemical shift evolution at the end of the t_1 period is required solely to ensure zero phase correction in the projected dimension, thus $\delta = \tau_{90}^N + 2$ µs (with τ_{90}^N being the ^{15}N 90° pulse length and 2 µs the minimal delay between two pulses). (**b**) for angles α above 45° the period 2τ is first used for ^{1}H single quantum (SQ) evolution in constant time manner (Bazzo et al. 2001; Ying et al. 2007) with $\Delta = t_2/2 - t_1/2 - \tau_{90}^N - \delta$ (while $\delta = \tau_{90}^N + 2$ µs). When the SQ time period is used up completely, i.e. $t_2/2 > t_1/2 + \delta + 2\tau + \tau_{90}^N - \tau_{90}^H - \tau_{180}^{H_2O} - \tau_{G1}$ (τ_{90}^H = duration of the ^{1}H 90° pulse, $\tau_{180}^{H_2O}$ = duration of selective 180° pulse on water, τ_{G1} = duration of gradient G_1 including gradient recovery delay), additional proton evolution is realized by increasing δ such that $\delta = t_2/2 - t_1/2 - \tau_{90}^N - 2\tau + \tau_{180}^{H_2O} + \tau_{G1} + \tau_{90}^H$. At the very beginning of the evolution time when $t_2/2 < t_1/2 + \delta + 2\tau_{90}^N + 2\mu$ the ^{15}N 180° pulse can not be centered with the ^{1}H 180° pulse; in this situation $\Delta = \tau_{90}^N + 2$ µs and the ^{1}H 180° pulse is moved independently of the ^{15}N 180° pulse. With the pulse sequence (**b**) a normal (unprojected) 3D NOESY spectrum can be recorded when the evolution times t_1 and t_2 are incremented independently

with respect to the ^{1}H axis in the indirect dimension, i.e. $\alpha = 0°$ corresponds to a conventional 2D [^{1}H,^{15}N]-HMQC-NOESY and $\alpha = 90°$ to a 2D ^{15}N-filtered [^{1}H, ^{1}H]-NOESY. For projection angles $0 \leq \alpha \leq 45°$ where the ^{1}H evolution period is shorter or equal to the ^{15}N evolution period, the pulse sequence in Fig. 1a is proposed. This sequence requires one additional 180° nitrogen pulse and no additional delays compared to the conventional experiment. The experimental scheme in Fig. 1b is proposed for projection angles above 45°, but it can be used for any projection angle. This sequence requires an additional ^{15}N 180° pulse and more elaborate programming for the implementation on a spectrometer. Both sequences include water flip-back pulses and magnetic field gradients which guarantee that the water magnetization stays along the positive z-axis during the whole experiment which is important for measurements with large molecular structures (Hiller et al. 2005b). The pulse sequence in Fig. 1b is very similar to the 3D MT-PARE-experiment proposed by Ying et al. (2007), but requires one ^{15}N 180° pulse less, still it can be used for recording conventional ^{15}N-resolved 3D [^{1}H,^{1}H]-NOESY experiments, since all combinations of ^{1}H and ^{15}N evolution times can be realized. In sequence Fig. 1b constant-time single quantum proton evolution is applied as discussed in Ying et al. (2007) using the magnetization transfer periods 2τ for ^{1}H chemical shift evolution. This enables the acquisition of spectra with projection angles up to $\alpha \leq \arctan\left[1 + \left(1/J_{HN} - 2\tau_{180}^{H_2O} - 2\tau_{G1}\right)\Big/ t_{\max}\right]$ which have the same relaxation as the corresponding conventional 2D experiment (t_{max} is the maximal nitrogen evolution period and $\tau_{180}^{H_2O}$ the length of the selective ^{1}H 180° pulse on the water resonance and τ_{G1} the length of the gradient, including the recovery delay, applied during the ^{1}H-^{15}N transfer period). Quadrature detection and the separation of the two sub-spectra is obtained as described by Brutscher et al. (1995) using the pulse phases φ_1 and φ_2. The two resulting sub-spectra contain the amide resonances with frequencies in the indirect dimension of $\Omega_{H/N} = \Omega_N \cos\alpha + \Omega_H \sin\alpha$ and $\Omega_{H/N} = \Omega_N \cos\alpha - \Omega_H \sin\alpha$, respectively; where Ω_N and Ω_H are the ^{15}N and ^{1}H frequencies of the amide moiety.

For minimal spectral width in the indirect dimension the proton carrier frequency should be set in the middle of the amide region for the first part of the pulse sequences in

Fig. 1 and to the water frequency starting in the mixing time for the rest of the sequence including acquisition. The first three off-resonance water flip-back pulses have to be adjusted separately in this case. Alternatively, the carrier frequency can be set to the water resonance for the whole sequence which makes the adjustment of flipback pulses easier but increases the required sweep width in the indirect dimension. However, when applied to large molecular systems many transients per time increment are normally recorded and thus by reducing the number of transients and by a concomitant increase of the number of sampled time domain points the desired resolution can easily be maintained; alternatively an optimal sweep width can be calculated for a convenient folding of signals in both sub-spectra.

When applying the experimental schemes shown in Fig. 1 the projection angle α must be chosen such that on the one hand the frequency difference(s) of NOE cross peak(s) from the corresponding direct correlation peak(s) and on the other hand the frequency differences to other NOE cross peaks and direct correlation peaks are maximized. E.g., for the observation of one specific pair of NOEs between two amide resonances with the chemical shift differences $\Delta\Omega_H$ and $\Delta\Omega_N$ the separation is maximal at an angle $\alpha = \arctan(\Delta\Omega_H/\Delta\Omega_N)$; for resonances with degenerate ^{15}N-shifts and different ^{1}H-shifts maximum separation will occur at angles α close to 90°. However, for large molecules where relaxation must be minimized, the proton evolution period should not exceed the nitrogen evolution period and thus α should be chosen $\leq$45° for the sequence in Fig. 1a (or $\leq \arctan\left[1 + \left(1/J_{HN} - 2\tau_{180}^{H_2O} - 2\tau_{G1}\right)\Big/ t_{\max}\right]$ for the sequence in Fig. 1b). At projection angles close to 45° the experiment provides the maximal resolution for a given total maximal evolution time.

Projecting a spectrum with a projection angle α different from zero or a multiple of 90° results in a loss of $\sqrt{2}$ in signal-to-noise because two spectra with the frequency combinations $\Omega_{H/N} = \Omega_N \cos\alpha + \Omega_H \sin\alpha$ and $\Omega_{H/N} = \Omega_N \cos\alpha - \Omega_H \sin\alpha$ are obtained. This is a general drawback of reduced dimensionality experiments which, however, is offset by the fact that the signals have different relative positions in each projection and compared to the conventional 2D spectrum more cross peaks will be resolved. In the proposed experiment full sensitivity can be recovered by adding the two ^{1}H cross sections through the positions of each of the two amide resonances participating in an NOE interaction; this procedure increases the sensitivity by $\sqrt{2}$ since the noise at the position of two corresponding NOE cross peaks is not correlated. In this situation a 2D projection of a 3D HMQC-NOESY spectrum recorded with the sequence in Fig. 1a becomes more sensitive than any 3D spectrum including spectra recorded with the sequence in Fig. 1b where for proton evolution periods exceeding the ones of nitrogen by more than 5–6 ms additional periods with transverse proton magnetization have to be introduced.

Results and discussion

The H1 linker histone protein

In eukaryotic cells DNA is packed in DNA-histone complexes (nucleosomes). The X-ray structures of the nucleosome core particle and of its superstructure, the tetranucleosome, have been published (Luger et al. 1997; Schalch et al. 2005) but the positioning of the linker histone H1 in the nucleosome as well as its role in regulation of gene expression is still a puzzle. The chicken H1 linker histone protein used in this study has a total molecular weight of 22.6 kDa (Hartman et al. 1977). It comprises a central globular domain with 75 amino acids, for which an NMR structure is available (Cerf et al. 1994), and flexible amino- and carboxy-terminal domains with 39 and 111 amino acids, respectively. The central globular domain was shown to be essential for H1 binding and its positioning in the nucleosome (Allan et al. 1980; Vermaak et al. 1998); the terminal domains seem to be important for the H1-induced chromatin compaction (Allan et al. 1986; Hendzel et al. 2004). The C-terminal domain acquires α-helical structure upon interaction with DNA (Clark et al. 1988; Hill et al. 1989; Vila et al. 2000, 2001) and is mainly responsible for the chromatin compaction (Lu and Hansen 2004). The N-terminal domain is believed to be involved in the location and anchoring of the globular domain to the nucleosome (Allan et al. 1986). Another study suggests that a helix-turn-helix secondary structure element with a Gly–Gly motif in the turn (Vila et al. 2002) is induced in the N-terminal domain upon binding to DNA.

The chicken H1 sequence contains 12 glycine residues; two of them (Gly32 and Gly33) are sequential neighbors in the N-terminal domain and the other 10 are situated in the globular domain. The N-terminal Gly–Gly motif, conserved in many vertebrate H1 subtypes, is believed to provide the orientational freedom required for tracking of the phosphate backbone of the linker DNA by the two helices or for the simultaneous binding of nucleosomal and linker DNA (Vila et al. 2002). In summary, the Gly–Gly motif appears to be a functionally important site and its characterization by NMR could provide new details about DNA-binding by H1. For such studies the Gly–Gly motif must be assigned in the complex with DNA which was achieved using the projected [^{1}H,^{15}N]-HMQC-[^{1}H,^{1}H]-NOESY experiment (Fig. 1a).

Observation of NOEs in the 121.3 kDa H1-DNA complex

A [^{1}H,^{15}N]-correlation NMR spectrum of free ^{15}N-labeled H1 in solution (data not shown) shows a set of well dispersed signals from a folded domain and a large number of narrow lines in the random coil region of the spectrum apparently arising from the unstructured terminal domains. Assignment of most of these poorly dispersed resonances seems hardly possible due to extreme overlap and will become even more difficult in the complex of H1 with DNA. Despite the overlap, all 12 Gly resonances can be observed at the specific nitrogen chemical shift around 105 ppm. We could unambiguously distinguish the amide signals of the two sequential glycines from the N-terminal part in the spectra based on their negative heteronuclear NOE values (data not shown), the other 10 Gly residues located in the globular domain have positive values.

After binding of ^{15}N-labeled H1 to an unlabeled 152 base pair linear DNA duplex in a 1:1 molar ratio only a few resolved amide signals with low dispersion in the $^{1}H^{N}$ dimension remain observable in a [^{1}H,^{15}N]-correlation spectrum. The resonances from structured regions are broadened beyond detection, indicating either strong binding to DNA or intermediate timescale dynamics due to exchange between different conformations of H1 in the complex. The observable amide resonances correspond to residues from more flexible regions of the H1 protein, which do not strongly interact with DNA or the globular domain of H1. However, even these resonances show a substantial increase of the line width as a result of slower overall tumbling and/or chemical/conformational exchange. Two resonances with Gly-specific chemical shifts are among the observable signals in the H1-DNA complex (Fig. 2) and supposedly originate from Gly32 and Gly33 in the N-terminal tail, since the Gly residues in the globular domain cannot be observed. The observation of an NOE between the amide protons of these two residues would provide evidence for their sequential neighborhood and thus a basis for their assignment in the complex. In addition, the NOE intensity is related to the dynamics of Gly–Gly turn and can be used to characterize the rigidity of this region in different DNA-complexes, e.g. with linear versus supercoiled DNA. Due to the almost degenerate ^{15}N chemical shifts of the two Gly resonances a 2D ^{15}N-resolved [^{1}H,^{1}H]-NOESY cannot resolve the NOEs in the presence of much more intense direct correlation peaks. Moreover, these particular NOEs are expected to be weak due to the flexible nature of the Gly–Gly motif. Also in a 2D [^{1}H,^{1}H]-NOESY spectrum the weak NOEs would be too close to the diagonal to be resolved and could not be unambiguously distinguished from other NOE signals. Indeed no NOE between the two glycine amides could be observed in former NMR studies of the N-terminal H1 peptide (Vila et al. 2002) because of reported overlap.

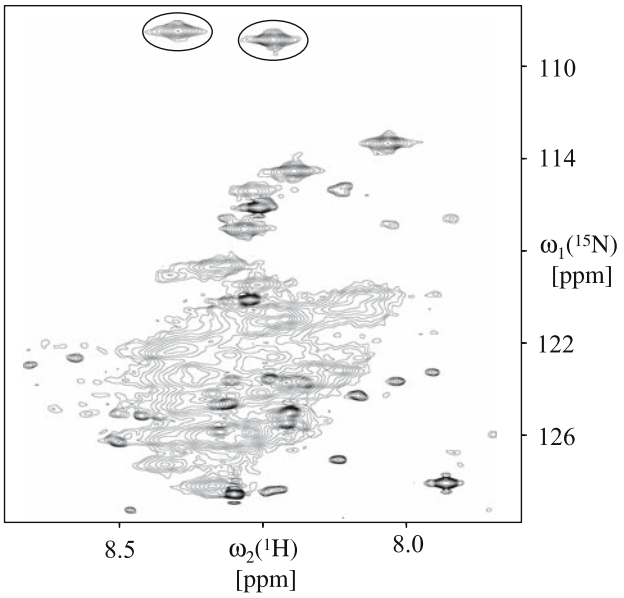

Fig. 2 [^{1}H,^{15}N]-HMQC spectrum of ^{15}N-labeled histone H1 in complex with a 152 bp DNA measured at 298 K on a Bruker DRX 750 MHz spectrometer equipped with a triple resonance probe with shielded z-gradient coil. The total evolution time on nitrogen was 43 ms. The complex with a molecular weight of 121.3 kDa was dissolved at a concentration of 125 μM in 95%/5% H_2O/D_2O at pH 6 containing 10 mM TRIS buffer, 0.1 mM EDTA and 50 mM NaCl. Only amides of mobile residues of H1 lead to observable resonances, signals from rigid regions of the complex are broadened beyond detection. Two Gly amide resonances with very similar ^{15}N chemical shifts are circled. The two corresponding Gly residues are suspected sequential neighbors, but in conventional spectra the sequential amide–amide NOEs cannot be resolved due to overlap with the very intense direct correlation peaks

The projected [^{1}H,^{15}N]-HMQC-[^{1}H,^{1}H]-NOESY experiment described in Fig. 1 was used to separate the NOE crosspeaks from the direct correlation peaks of amide protons of two potentially sequential glycine residues (Fig. 3). This NOE confirms that the corresponding resonances belong indeed to the glycines 32 and 33 in the amino-terminal domain of the 121.3 kDa histone H1-DNA complex. The spectrum shown in Fig. 3a was measured with a NOESY mixing time of 120 ms; the control spectrum in Fig. 3b with a mixing time of 5 ms shows no NOEs. The spectra in Fig. 3 were measured with a ratio of 0.4 ($\alpha = 21.8°$) between the two simultaneously incremented ^{1}H and ^{15}N evolution periods. The frequency difference between the Gly signals is enlarged in the projected 2D spectrum with respect to the conventional 2D [^{1}H,^{15}N]-correlation spectrum and the NOEs can be separated already at a low spectral resolution, such that the maximum evolution time could be reduced to 15.8 ms to increase sensitivity. The spectral width and the ^{15}N-carrier offset were chosen such that the Gly signals from the

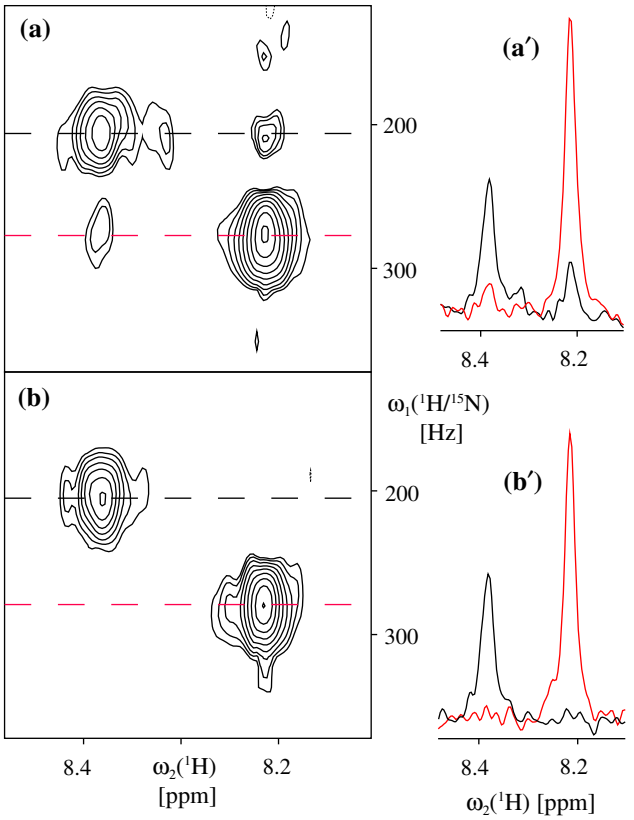

Fig. 3 Expanded spectral regions of a projected [^{1}H,^{15}N]-HMQC-[^{1}H,^{1}H]-NOESY measured at 750 MHz with a projection angle of +21.8° of the 121.3 kDa histone H1-DNA complex characterized in the caption of Fig. 2. The spectral region of the two glycine amide resonances marked in Fig. 2 is shown for two mixing times: (**a**) 120 ms and (**b**) 5 ms. The spectra were recorded with 30 hypercomplex sampling points (see caption Fig. 1) in the mixed ^{1}H–^{15}N indirect time domain, with a maximum evolution time of 15.8 ms on nitrogen and 6.3 ms on proton. 1500 scans per FID have been acquired resulting in 2.5 days of measurement time. The ^{1}H carrier was set to 4.7 ppm during the whole experiment. Selective pulses applied to the water resonance were carefully adjusted in power and phase and the relative amount of water magnetization retained along the +*z*-axis at the end of the experiment was measured by a tap-pulse (Hiller et al. 2005b) to be ~75% in steady-state. 30 complex points were linear predicted in the indirect dimension during processing. The horizontal broken lines in spectra (**a**) and (**b**) indicate the position of the cross-sections shown in corresponding colors in panels (**a′**) and (**b′**), respectively

positive angle projection were folded into the middle of the spectrum.

Conclusions

In this publication we have introduced and applied a relaxation optimized 2D experimental scheme for ^{15}N-labeled proteins that can resolve NOE signals that are overlapped in conventional 2D experiments. The application to a 121 kDa protein-DNA complex showed that the experiment provides a simple and effective technique for observation of NOE interactions between amide protons with degenerate ^{15}N-shifts in large molecules. The 2D projection experiment discussed in this paper can be used as a building block for the development of projection experiments based on 4D doubly ^{15}N- or simultaneously [^{13}C,^{15}N]-resolved [^{1}H,^{1}H]-NOESY pulse sequences.

Acknowledgements We thank Dr. Fred Damberger for technical discussions. This work was supported by "Schweizerischer Nationalfonds" (project 3100A0-113730) and by ETH Research Grant TH -42/04-2.

References

Allan J, Hartman PG, Cranerobinson C, Aviles FX (1980) The structure of histone-H1 and its location in chromatin. Nature 288:675–679

Allan J, Mitchell T, Harborne N, Bohm L, Crane-Robinson C (1986) Roles of H1 domains in determining higher order chromatin structure and H1 location. J Mol Biol 187:591–601

Bazzo R, Barbato G, Cicero DO (2001) Improved sensitivity in indirect monitoring of chemical shifts of proton-heteronuclear spin pairs (H-1-C-13 and H-1-N-15) in 3D and 4D NMR spectroscopy. J Biomol NMR 19:261–266

Bracewell RN (1956) Strip integration in radio astronomy. Austr J Phys 9:198–217

Brutscher B, Morelle N, Cordier F, Marion D (1995) Determination of an initial set of noe-derived distance constraints for the structure determination of N-15/C-13-labeled proteins. J Magn Reson Ser B 109:238–242

Cerf C, Lippens G, Ramakrishnan V, Muyldermans S, Segers A, Wyns L, Wodak SJ, Hallenga K (1994) Homo- and heteronuclear two-dimensional NMR studies of the globular domain of histone H1: full assignment, tertiary structure, and comparison with the globular domain of histone H5. Biochemistry 33:11079–11086

Christodoulou J, Larsson G, Fucini P, Connell SR, Pertinhez TA, Hanson CL, Redfield C, Nierhaus KH, Robinson CV, Schleucher J et al (2004) Heteronuclear NMR investigations of dynamic regions of intact *Escherichia coli* ribosomes. Proc Natl Acad Sci USA 101:10949–10954

Clark DJ, Hill CS, Martin SR, Thomas JO (1988) Alpha-helix in the carboxy-terminal domains of histones H1 and H5. EMBO J 7:69–75

Eghbalnia HR, Bahrami A, Tonelli M, Hallenga K, Markley JL (2005) High-resolution iterative frequency identification for NMR as a general strategy for multidimensional data collection. J Am Chem Soc 127:12528–12536

Fiaux J, Bertelsen EB, Horwich AL, Wuthrich K (2002) NMR analysis of a 900K GroEL-GroES complex. Nature 418:207–211

Grzesiek S, Bax A (1993) Amino-acid type determination in the sequential assignment procedure of uniformly C-13/N-15-enriched proteins. J Biomol NMR 3:185–204

Hartman PG, Chapman GE, Moss T, Bradbury EM (1977) Studies on the role and mode of operation of the very-lysine-rich histone H1 in eukaryote chromatin. The three structural regions of the histone H1 molecule. Eur J Biochem 77:45–51

Hendzel MJ, Lever MA, Crawford E, Th'ng JP (2004) The C-terminal domain is the primary determinant of histone H1 binding to chromatin in vivo. J Biol Chem 279:20028–20034

Hill CS, Martin SR, Thomas JO (1989) A stable alpha-helical element in the carboxy-terminal domain of free and chromatin-bound histone H1 from sea urchin sperm. EMBO J 8:2591–2599

Hiller S, Fiorito F, Wuthrich K, Wider G (2005a) Automated projection spectroscopy (APSY). Proc Natl Acad Sci USA 102:10876–10881

Hiller S, Wider G, Etezady-Esfarjani T, Horst R, Wuthrich K (2005b) Managing the solvent water polarization to obtain improved NMR spectra of large molecular structures. J Biomol NMR 32:61–70

Horst R, Bertelsen EB, Fiaux J, Wider G, Horwich AL, Wuthrich K (2005) Direct NMR observation of a substrate protein bound to the chaperonin GroEL. Proc Natl Acad Sci USA 102:12748–12753

Horst R, Wider G, Fiaux J, Bertelsen EB, Horwich AL, Wuthrich K (2006) Proton-proton Overhauser NMR spectroscopy with polypeptide chains in large structures. Proc Natl Acad Sci USA 103:15445–15450

Kim S, Szyperski T (2003) GFT NMR, a new approach to rapidly obtain precise high-dimensional NMR spectral information. J Am Chem Soc 125:1385–1393

Kozminski W, Zhukov I (2003) Multiple quadrature detection in reduced dimensionality experiments. J Biomol NMR 26: 157–166

Kupče E, Freeman R (2003) Projection-reconstruction of three-dimensional NMR spectra. J Am Chem Soc 125:13958–13959

Kupče E, Freeman R (2004) Projection-reconstruction technique for speeding up multidimensional NMR spectroscopy. J Am Chem Soc 126:6429–6440

Kupče E, Freeman R (2005) Resolving ambiguities in two-dimensional NMR spectra: the 'TILT' experiment. J Magn Reson 172:329–332

Kupče E, Nishida T, Widmalm G, Freeman R (2005) Resolving overlap in two-dimensional NMR spectra: nuclear Overhauser effects in a polysaccharide. Magn Reson Chem 43:791–794

Lu X, Hansen JC (2004) Identification of specific functional subdomains within the linker histone H10 C-terminal domain. J Biol Chem 279:8701–8707

Luger K, Mader AW, Richmond RK, Sargent DF, Richmond TJ (1997) Crystal structure of the nucleosome core particle at 2.8 A resolution. Nature 389:251–260

Malmodin D, Billeter M (2005) Signal identification in NMR spectra with coupled evolution periods. J Magn Reson 176:47–53

Nagayama K, Bachmann P, Wuthrich K, Ernst RR (1978) Use of cross-sections and of projections in 2-dimensional nmr-spectroscopy. J Magn Reson 31:133–148

Pervushin K, Eletsky A (2003) A new strategy for backbone resonance assignment in large proteins using a MQ-HACACO experiment. J Biomol NMR 25:147–152

Schalch T, Duda S, Sargent DF, Richmond TJ (2005) X-ray structure of a tetranucleosome and its implications for the chromatin fibre. Nature 436:138–141

Shon K, Opella SJ (1989) Detection of H-1 homonuclear noe between amide sites in proteins with H-1/N-15 heteronuclear correlation spectroscopy. J Magn Reson 82:193–197

Sprangers R, Kay LE (2007) Quantitative dynamics and binding studies of the 20S proteasome by NMR. Nature 445:618–622

Szyperski T, Wider G, Bushweller JH, Wuthrich K (1993a) 3d C-13-N-15-heteronuclear 2-spin coherence spectroscopy for polypeptide backbone assignments in C-13-N-15-double-labeled proteins. J Biomol NMR 3:127–132

Szyperski T, Wider G, Bushweller JH, Wuthrich K (1993b) Reduced dimensionality in triple-resonance nmr experiments. J Am Chem Soc 115:9307–9308

Tugarinov V, Choy WY, Kupče E, Kay LE (2004) Addressing the overlap problem in the quantitative analysis of two dimensional NMR spectra: Application to N-15 relaxation measurements. J Biomol NMR 30:347–352

Vermaak D, Steinbach OC, Dimitrov S, Rupp RAW, Wolffe AP (1998) The globular domain of histone H1 is sufficient to direct specific gene repression in early Xenopus embryos. Curr Biol 8:533–536

Vila R, Ponte I, Collado M, Arrondo JL, Suau P (2001) Induction of secondary structure in a COOH-terminal peptide of histone H1 by interaction with the DNA: an infrared spectroscopy study. J Biol Chem 276:30898–30903

Vila R, Ponte I, Jimenez MA, Rico M, Suau P (2000) A helix-turn motif in the C-terminal domain of histone H1. Protein Sci 9: 627–636

Vila R, Ponte I, Jimenez MA, Rico M, Suau P (2002) An inducible helix-Gly-Gly-helix motif in the N-terminal domain of histone H1e: a CD and NMR study. Protein Sci 11:214–220

Ying JF, Chill JH, Louis JM, Bax A (2007) Mixed-time parallel evolution in multiple quantum NMR experiments: sensitivity and resolution enhancement in heteronuclear NMR. J Biomol NMR 37:195–204